

See discussions, stats, and author profiles for this publication at: <https://www.researchgate.net/publication/245292789>

# Exterior Reflections in Elliptic Harbor Wave Models

Article in *Journal of Waterway, Port, Coastal and Ocean Engineering* · May 1996

DOI: 10.1061/(ASCE)0733-950X(1996)122:3(118)

CITATIONS

52

READS

39

3 authors, including:



[Vijay Panchang](#)

Texas A&M University - Galveston

49 PUBLICATIONS 1,161 CITATIONS

[SEE PROFILE](#)



[Zeki Demirebilek](#)

Engineer Research and Development Center - U.S. Army

175 PUBLICATIONS 2,023 CITATIONS

[SEE PROFILE](#)

Some of the authors of this publication are also working on these related projects:



Estimating runup using 1D and 2D Boussinesq model [View project](#)



Eagle Harbor [View project](#)

# EXTERIOR REFLECTIONS IN ELLIPTIC HARBOR WAVE MODELS

By Bingyi Xu,<sup>1</sup> Student Member, ASCE, Vijay Panchang,<sup>2</sup> Member, ASCE,  
and Zeki Demirebilek,<sup>3</sup> Member, ASCE

**ABSTRACT:** Traditional elliptic harbor wave models are based on the assumptions that the exterior sea region (i.e. the region outside the computational grid) is of constant depth and that the exterior coastlines are collinear and fully reflecting. This paper demonstrates that for most coastal regions, where these assumptions are generally not true, their effect on model results is substantial. This leads to unreliable simulations. Enlarging the model domain to overcome their effects is cumbersome and often prohibitive. To overcome these difficulties, the use of parabolic approximations of the mild-slope wave equation as open boundary conditions is explored. Suitable parabolic equations are derived and interfaced with an elliptic finite-element model. Since the parabolic approximation does not describe wave scattering as rigorously as the traditional method, the new model is tested against analytical and other solutions for cases where scattering is extensive. Errors resulting from the parabolic approximation are found to be extremely small. Further model tests show that for the generally realistic case where exterior reflection coefficients are less than unity, the new method requires considerably smaller domains than the traditional method, resulting in reduced modeling effort. The model is also applied to Toothacher Bay, Maine, and the use of the parabolic boundary conditions eliminates many spurious features in the simulation.

## INTRODUCTION

The solution of the two-dimensional elliptic mild-slope wave equation is a well-accepted method for modeling surface gravity waves in harbors (Chen and Houston 1987; Chen 1990; Xu and Panchang 1993; Mei 1983; Berkhoff 1976; Kostense et al. 1986; Tsay and Liu 1983). This equation may be written as

$$\nabla \cdot (CC_g \nabla \phi) + \frac{C_g}{C} \sigma^2 \phi = 0 \quad (1)$$

where  $\phi(x, y)$  = complex surface elevation function, from which the wave height can be estimated;  $\sigma$  = wave frequency under consideration;  $C(x, y)$  = phase velocity =  $\sigma/k$ ;  $C_g(x, y)$  = group velocity =  $\partial\sigma/\partial k$ ;  $k(x, y)$  = wave number ( $=2\pi/L$ ), related to the local depth  $d(x, y)$  through the dispersion relation

$$\sigma^2 = gk \tanh(kd) \quad (2)$$

Eq. (1) is usually solved by numerical techniques after separating the overall domain into two regions (see Fig. 1): the interior harbor area  $\Omega$ , which is usually covered by a finite-element or finite-difference grid, and the exterior sea  $\Omega'$  which is often called the "superelement." In the exterior, the wavefield  $\phi_{\text{ext}}$  consists of the specified incident wavefield  $\phi_i$ , reflected wavefield  $\phi_r$ , and the scattered wavefield  $\phi_s$ . For the numerical solution, analytical descriptions of all three are required. For clarity, these are presented in Appendix I. The solutions in the interior and the exterior are then matched and the overall wavefield determined via a numerical algorithm (Mei 1983; Xu and Panchang 1993).

The scattered wavefield  $\phi_s$  that stems from the existence of the harbor is of particular interest. The classical representation of  $\phi_s$  is

$$\phi_s = \sum_{n=0}^{\infty} H_n(kr)(A_n \cos n\theta + B_n \sin n\theta) \quad (3)$$

where  $(r, \theta)$  = location of a point in polar coordinates;  $k$  = wave number;  $H_n$  = Hankel function of the first kind and order  $n$ ; and  $A_n$  and  $B_n$  = unknown coefficients. [It may be noted that an open boundary of semicircular shape, while not essential, greatly facilitates the application of (3) in finite-element models.] Although the classical method results in (3) which rigorously satisfies the governing (1) and the Sommerfeld radiation condition, it has three limitations: (1) The exterior region must have a constant depth; (2) the exterior coastlines  $A_1D_1$  and  $A_2D_2$  must be collinear; and (3) the exterior coastlines  $A_1D_1$  and  $A_2D_2$  must be fully reflecting. (This is proved in Appendix I.) These requirements usually cannot be met for most coastal domains where the exterior geometry varies arbitrarily, and the unrealistic bathymetric representation used perforce by the modeler invariably has an adverse influence on the solution. Limitation (3) is particularly troublesome; an example is provided in Fig. 2, where the results of applying a finite-element model (called "CGWAVE" and described later) to Toothacher Bay, Maine, are shown. While these results constitute the correct solution of the problem solved, the simulation yields extremely large amplification factors and rapid variations in the wave pattern in the outer regions of the domain. These effects, which are primarily due to a fully reflected wavefield generated from the exterior coastline, would clearly be spurious in case of exterior coastlines with low reflectivity. We have also observed them in several harbor simulations while using the model HARBD (Chen and Houston 1987). One may of course enlarge the interior region in the hope that these effects do not contaminate the results in the area of interest; however, there is no guarantee that these effects are confined to specific regions. In addition, the extra memory requirements and grid generation for a larger domain are usu-

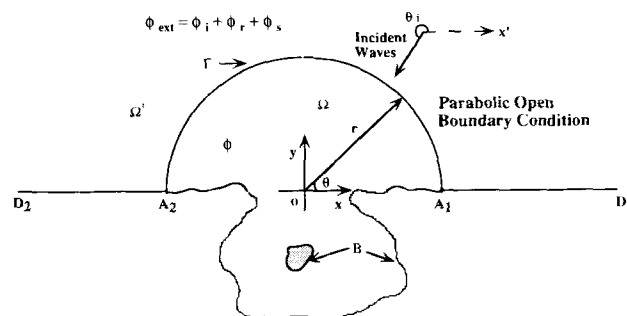


FIG. 1. Harbor Wave Model Domain

<sup>1</sup>Grad. Res. Asst., Dept. of Civ. Engrg., Univ. of Maine, Orono, ME 04469-5706.

<sup>2</sup>Assoc. Prof., Dept. of Civ. Engrg., Univ. of Maine, Orono, ME.

<sup>3</sup>Res. Hydr. Engr., U.S. Army Engr. Wtrwy. Experiment Station, Coast. Engrg. Res. Ctr., Vicksburg, MS 39180-6199.

Note. Discussion open until November 1, 1996. To extend the closing date one month, a written request must be filed with the ASCE Manager of Journals. The manuscript for this paper was submitted for review and possible publication on October 18, 1994. This paper is part of the *Journal of Waterway, Port, Coastal, and Ocean Engineering*, Vol. 122, No. 3, May/June, 1996. ©ASCE, ISSN 0733-950X/96/0003-0118-0126/\$4.00 + \$.50 per page. Paper No. 9440.

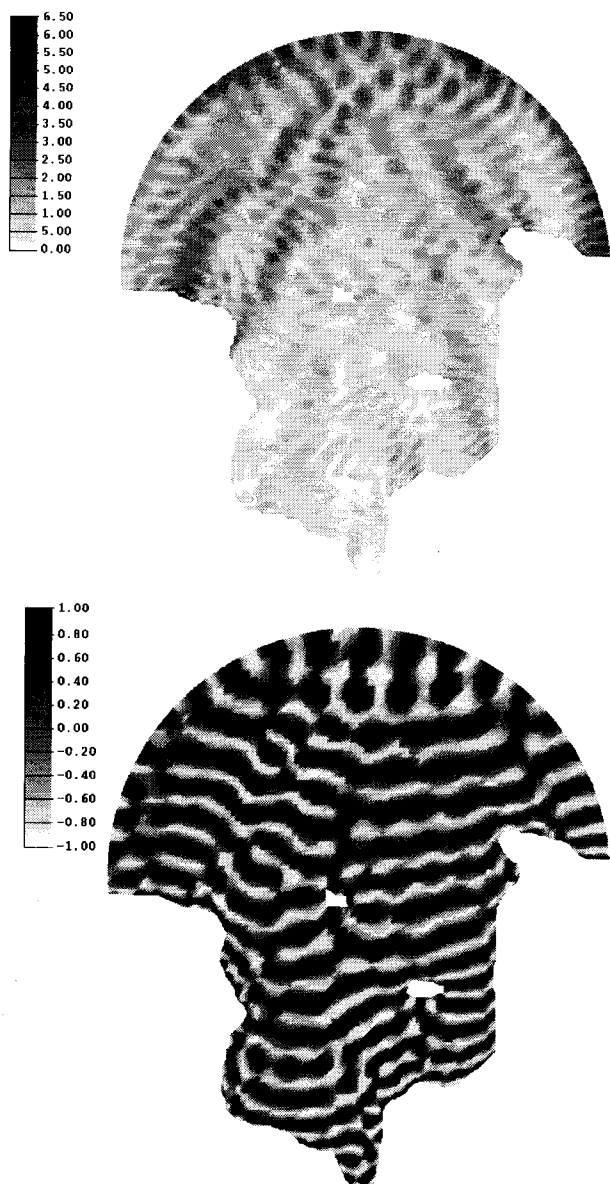


FIG. 2. Model Simulation in Toothacher Bay via Traditional Approach (20-s Waves Incident from Top—See Also Figs. 12 and 13): (a) Amplification Factors; (b) Cosine of Phase Angle

ally exceedingly demanding. Use of (3) thus renders the application of harbor wave models problematic.

To overcome these difficulties, Panchang et al. (1993) have described a procedure that requires the exterior domain to be suitably divided into a finite number of regions of constant depths. A boundary integral equation is then developed for each of these exterior regions using the appropriate Green's function. The boundary element formulations for these regions are then matched with each other along the interfaces and with the finite-element network in the model interior to obtain the solution. It was found, however, that this type of model is extremely cumbersome to code and construct for general implementation. Other difficulties may also be expected if mechanisms such as dissipation, wave-current interaction, etc. are to be introduced into the governing equation. Chen (1990) also has suggested discretizing the exterior domain into a finite number of radial "infinite elements" with a prespecified shape function in each element. However, this shape function is entirely dependent on the farfield approximation for the Hankel functions, suggesting that a fairly large computational domain is still needed. Also, no detailed comparisons for the case of

low exterior reflectivities have been provided to assess the advantages of this method.

In this paper we develop an alternative method for dealing with the open boundary of elliptic wave models so that the case of arbitrary reflections from straight exterior coastlines can be handled. Although this strictly eliminates limitation (3) of the classical method, exterior coastlines of arbitrary shape may also be permitted [i.e. limitation (2)] if they have low reflectivity. The approach is based on the strategy originally proposed by Kirby (1989) in the context of rectangular finite-difference domains studied by Panchang et al. (1988); it involves the use of the "parabolic approximation" of the mild-slope wave equation as the open boundary condition for the scattered waves. The parabolic approximation allows only forward propagation with weak lateral scattering, i.e. it can accommodate waves exiting the domain through a limited aperture of approximately  $45^\circ$  about a dominant direction. However, the dominant direction of the scattered outgoing waves is not known a priori; what is known is that they must propagate radially out to infinity to satisfy the Sommerfeld radiation condition. To tackle this situation within the artifice of the parabolic approximations, we may reasonably select a scattering center [e.g. by assuming that most of the scattering originates within the harbor itself (region  $\Omega$ ) and/or by a group of scattering structures, islands, etc.] and use a circular segment around it as the open boundary. The dominant direction of the outgoing waves may then be assumed to be largely the radial direction at each point of the open boundary. Accordingly, parabolic approximations in radial coordinates are derived and applied along a circular segment that is used to separate the interior computational domain from the exterior sea.

This approach thus represents a compromise between the rigor of the conventional method represented by (3) and its limitations. Eq. (3) is rigorous as far as wave scattering directions are concerned since it is a complete solution of (1). However, it places unrealistic requirements on the exterior bathymetric geometry that adversely impact model solutions. The proposed approach is somewhat approximate insofar as the scattered wave angles are concerned: all waves scattered from the region  $\Omega$  may not be radially incident on the open boundary. However, the treatment of the scattered waves in this approach requires no assumptions regarding the bathymetry and allows the modeler greater flexibility while tackling realistic domains. In addition, it may be hoped that the approximations will have limited negative influence since they pertain only to one component of the overall exterior wavefield (viz. the scattered potential).

The layout of the paper is as follows. In the next section, parabolic equations appropriate for use with the elliptic wave model are developed. The following section provides the variational formulation used to construct a finite-element model with the parabolic boundary conditions. Verification of this procedure and comparison with the conventional method are then described. Finally, concluding remarks are provided.

## PARABOLIC APPROXIMATIONS FOR OPEN BOUNDARY CONDITION

To obtain parabolic approximations of the mild-slope wave equation, (1), it is helpful to first transform it as follows (Radder 1979):

$$\nabla^2 \Phi + K^2 \Phi = 0 \quad (4)$$

via the relations

$$\Phi = \sqrt{CC_g} \phi \quad \text{and} \quad K^2 = k^2 - \frac{\nabla^2 \sqrt{CC_g}}{\sqrt{CC_g}} \quad (5)$$

Parabolic approximations for (4) in non-Cartesian (nonorthog-

onal) coordinate systems have been studied by Tsay and Liu (1982), Isobe (1986), Liu and Boissevain (1988), and Kirby (1988). However, their developments are not directly applicable to the problem described previously. To obtain a parabolic equation suitable for application along a circular segment, we use a polar coordinate system; (4) then becomes:

$$\Phi_{rr} + \frac{1}{r} \Phi_r + \frac{1}{r^2} \Phi_{\theta\theta} + K^2 \Phi = 0 \quad (6)$$

(Our goal is to derive a parabolic approximation only for the scattered waves which originate from the interior. It must therefore be noted that the following development pertains to  $\Phi_s$ .)

As stated earlier, (3) is a rigorous solution of (6) for  $K = k = \text{constant}$ ; its far-field approximation is

$$\Phi(r, \theta) \sim \sum_{n=0}^{\infty} A_n(\theta) \sqrt{\frac{2}{\pi k_0 r}} \exp \left\{ i \left[ k_0 r - \left( n + \frac{1}{2} \right) \frac{\pi}{2} \right] \right\} \quad (7)$$

where  $k_0$  refers to the constant depth in the exterior. Eq. (7) also completely satisfies the Sommerfeld radiation condition (as shown in Appendix I). However, it is accompanied by limitations on the exterior geometry. In the spirit of retaining the advantages (and hence the form) of (7) to the extent possible, for more general application, we choose the following solution:

$$\Phi(r, \theta) = \Psi(r, \theta) \frac{1}{\sqrt{k_0 r}} e^{ik_0 r} \quad (8)$$

where  $k_0$  may be suitably defined as some characteristic wave number along the open boundary. A parabolic approximation may now be derived in the usual way. Substituting (8) into (6), we have

$$\Psi_{rr} + 2ik_0 \Psi_r + \frac{1}{r^2} \Psi_{\theta\theta} + \left( K^2 - k_0^2 + \frac{1}{4r^2} \right) \Psi = 0 \quad (9)$$

The desired parabolic approximation may be obtained by dropping the  $\Psi_{rr}$  term (e.g. Kirby et al. 1994), i.e. diffraction effects in the  $r$ -direction are assumed to be weak. This yields [in conjunction with (5) and (8)]

$$\phi_r + p\phi + q\phi_{\theta\theta} = 0 \quad (10)$$

where

$$p = \frac{K^2 r^2 + k_0^2 r^2 + ik_0 r + 1/4}{2ik_0 r^2} \quad \text{and} \quad q = \frac{1}{2ik_0 r^2} \quad (11)$$

[In (10), local bathymetric variations, i.e.  $\partial\sqrt{CC_g}/\partial r$  and  $\partial\sqrt{CC_g}/\partial\theta$ , along the semicircle are ignored.] Eq. (10) may also be obtained via the splitting matrix method (Radder 1979).

It must be noted that the parabolic approximation (10) is not unique; indeed, there are several ways to derive such approximations and they result in different equations (Kirby 1986a,b; Kirby et al. 1994). The prior development is essentially based on the assumption (8), which can be justified only on heuristic grounds; the scattered waves propagate out in the  $r$ -direction [as indicated by  $\exp(ik_0 r)$ ] and decrease in amplitude as  $r^{-1/2}$  (as required by energy conservation). While these properties are strictly true only in the far field, they are desirable in the near field (just beyond the open boundary). They are hence retained in (8), and variations from the exact form (7) are assumed to be contained only in the function  $\Psi(r, \theta)$ . Thus (8) may be viewed as a more general form of (7) for the purpose of developing a radiation boundary condition. Parabolic approximations similar to (10) have been derived recently by Kirby et al. (1994) for the comparable case of waves

propagating outwards between two diverging breakwaters. Unlike our formulation (8) and that of Kirby et al. (1994), the shape functions used by Chen (1990) for his radially diverging infinite elements do not contain the function  $\Psi(r, \theta)$ . They are thus strictly valid only in the farfield, in terms of  $r$ . Also, Chen (1990) has assumed that  $\phi$  varies linearly in the  $\theta$ -direction over an infinite element. This implies that  $\phi_{\theta\theta} = 0$  within the element, which is not very satisfying as  $r$  increases in the continuously expanding infinite element, since the theoretical requirement from (6) is  $\phi_{\theta\theta} = -n^2\phi$  (resulting from separation of variables).

Alternatively, the parabolic approximation may be based on a more conventional assumption. In Cartesian models, this assumption is

$$\Phi = \Psi(x, y)\exp(ik_0 x)$$

for waves propagating largely in the  $x$ -direction. The analogous form for our purpose would be

$$\Phi = \Psi(r, \theta)\exp(ik_0 r) \quad (12)$$

for waves propagating largely in the  $r$ -direction. The parabolic approximation that results is again (10) with

$$p = \frac{r(K^2 + k_0^2)}{1 + 2ik_0 r} \quad \text{and} \quad q = \frac{1}{r(1 + 2ik_0 r)} \quad (13)$$

While it is difficult to rigorously establish the superiority of one parabolic equation over the other, it would intuitively appear that (10) and (11) are preferable because (8) explicitly incorporates the desired radiation properties.

## FINITE-ELEMENT MODEL DEVELOPMENT

To solve (1), a finite-element grid is constructed within the model interior encompassed by a semicircular open boundary and the coastal boundaries. In the exterior, the total potential  $\Phi_{\text{ext}}$  may be written as

$$\Phi_{\text{ext}} = \phi_i + \phi_r + \phi_s = \phi_0 + \phi_s \quad (14)$$

where  $\phi_i$  = (specified) incident potential  $= A_i \exp[ikr \cos(\theta - \theta_i)]$ ;  $\phi_r$  = reflected potential due to the exterior coastline, which may be estimated as  $K_{re} A_i \exp[ikr \cos(\theta + \theta_i)]$  if the coastline is collinear with the  $x$ -axis and has a reflection coefficient  $K_{re}$ ; and  $\phi_s$  = scattered potential due to the harbor.

Along the (other solid) boundary  $B$  we have the following boundary condition:

$$\frac{\partial\phi}{\partial n} = \alpha\phi \quad \text{where} \quad \alpha = \frac{ik(1 - K_r)}{(1 + K_r)} \quad (15)$$

where the real quantity  $K_r$  denotes the (specified) reflection coefficient. Along the open boundary  $\Gamma$  we use (10) as the boundary condition for the scattered waves. Matching the potential and its normal derivative along  $\Gamma$  and using the parabolic open boundary condition (10), we have

$$\phi = \phi_0 + \phi_s \quad (16)$$

and

$$\frac{\partial\phi}{\partial n} = \frac{\partial\phi_0}{\partial r} + \frac{\partial\phi_s}{\partial r} = \frac{\partial\phi_0}{\partial r} - \left( p\phi_s + q \frac{\partial^2\phi_s}{\partial\theta^2} \right) \quad (17)$$

Using (16) to eliminate  $\phi_s$  yields

$$\frac{\partial\phi}{\partial n} = -p\phi - q \frac{\partial^2\phi}{\partial\theta^2} + g \quad (18)$$

where

$$g = \frac{\partial\phi_0}{\partial r} + p\phi_0 + q \frac{\partial^2\phi_0}{\partial\theta^2} \quad (19)$$

Eq. (1) is to be solved in the model interior using the boundary conditions (15) and (18). To use finite elements it is necessary to develop the equivalent variational problem on the appropriate functional. While this has been done for the conventional method using (3) (Mei 1983), the presence of the higher-order tangential derivative in (18) renders the development more complicated for the new method. For brevity we avoid this development and state that the desired functional is

$$J = \int_{\Omega} \frac{1}{2} \left[ CC_s (\nabla \phi)^2 - \frac{C_s}{C} \sigma^2 \phi^2 \right] dA - \int_B \frac{1}{2} \alpha CC_s \phi^2 ds - \int_{\Gamma} \frac{1}{2} CC_s \left[ 2g\phi - p\phi^2 + q \left( \frac{\partial \phi}{\partial \theta} \right)^2 \right] ds + \left( \frac{1}{2} \alpha CC_s q r^2 \phi^2 \right)_{at A_1} + \left( \frac{1}{2} \alpha CC_s q r^2 \phi^2 \right)_{at A_2} \quad (20)$$

where the last two terms are evaluated at the end points ( $A_1$  and  $A_2$ ) of the open boundary. It can be demonstrated that the variation of  $J$  is

$$\delta J = - \int_{\Omega} \delta \phi \left[ \nabla \cdot (CC_s \nabla \phi) + \frac{C_s}{C} \sigma^2 \phi \right] dA + \int_B \delta \phi CC_s \left( \frac{\partial \phi}{\partial n} - \alpha \phi \right) ds + \int_{\Gamma} \delta \phi CC_s \left( \frac{\partial \phi}{\partial n} + p\phi + q \frac{\partial^2 \phi}{\partial \theta^2} - g \right) ds - \left[ \delta \phi CC_s q r^2 \left( \frac{\partial \phi}{\partial n} - \alpha \phi \right) \right]_{at A_1} - \left[ \delta \phi CC_s q r^2 \left( \frac{\partial \phi}{\partial n} - \alpha \phi \right) \right]_{at A_2} \quad (21)$$

It is clear that  $\delta J$  will be zero if and only if, first,  $\phi$  satisfies the mild-slope equation in  $\Omega$ , and second,  $\phi$  satisfies the boundary conditions on both  $B$  and  $\Gamma$ .

If wave propagation around offshore islands or structures is to be considered in a domain with no other coastal boundaries (e.g. see the following model verification section), a full circle can be used as the open boundary  $\Gamma$ . It can then be shown that the functional in this case reduces to the first three terms of (10).

The finite-element solution now follows in the usual way (Mei 1983). In this study, simple triangular elements were used in conjunction with (20). Calculating the variation of  $J$  then leads to a system of linear equations (i.e.  $[A]\{\phi\} = \{f\}$ ) which is typically extremely large and hence difficult to solve. Iterative conjugate-gradient techniques developed by Panchang et al. (1991) were used to alleviate these difficulties. In fact, these techniques were found to be far more efficient in the present finite-element runs than for the finite-difference studies of Xu and Panchang (1993) and Panchang et al. (1991). Li (1994)

**TABLE 1. Comparison of Iterative Schemes Developed by Panchang et al. (1991) and Li (1994) (Residual Error =  $10^{-8}$ )**

No. (1)	No. of equations (2)	Iterations (Panchang et al. 1991) (3)	Iterations (Li 1994) (4)	CPU (s) (Panchang et al. 1991) (5)	CPU (s) (Li 1994) (6)
1	660	920	160	32.3	5.5
2	1,779	2,000	400	204.0	40.0
3	2,943	2,400	700	412.0	118.0
4	3,605	3,100	600	659.0	125.0
5	6,256	4,100	3,200	1,284.1	973.8

has recently suggested modifications to the iterative schemes of Panchang et al. (1991) to enhance convergence. These were also investigated for a rectangular harbor of varying size (cases 1–4 in Table 1) and for Toothacher Bay (case 5 in Table 1). Although these modifications resulted in faster convergence, it was noticed that unlike the basic procedures of Panchang et al. (1991), they do not converge to a solution monotonically. Instead, the residual error decreases in an oscillatory manner as the iterations proceed. Also, the gain in CPU time varies from case to case and appears to be problem-specific. A model (called CGWAVE) was developed using these iterative methods and interfaced with the grid-generator associated with the "FASTTABS" flow model (Jones and Richards 1992). These features enabled rapid simulations on domains containing several thousand triangular grids of varying size (based on the desired wave-length resolution). Two versions of the model, with the open boundary treated according to the traditional approach, (3), and according to the parabolic approximations, (10), (11), and (13), were constructed to facilitate comparison.

## MODEL VERIFICATION

To verify the new approach, the finite-element model CGWAVE was applied to two well-known test cases. The first was a simulation of wave propagation around a circular island situated on a paraboloidal shoal surrounded by a sea of constant depth (Fig. 3). This is a particularly rigorous test case for the new method, since analytical solutions for long waves (Homma 1950; Jonsson et al. 1976) indicate extensive scattering in all directions. Hitherto elliptic models have used the rigorous representation (3) to simulate such scattering (Xu and Panchang 1993; Houston 1981; Tsay and Lui 1983). Compared with these models, the new method relaxes the treatment of the scattered waves (to attain greater versatility), and the analytical solutions facilitate an examination of the effects of this relaxation.

A circular open boundary was placed at a distance of  $0.1L$  from the toe of the shoal, where  $L$  = incident wavelength. A triangular finite-element grid was constructed with the size of the triangles varying with the water depth; a resolution of approximately eight grids per (local) wavelength was used. For a wave period of  $T = 240$  s, this resulted in 609 linear equations. Modeled wave heights using (11) and (13) on the open boundary were essentially identical and are shown in the bottom half of Fig. 4. For comparison, the analytical results are shown in the top of Fig. 4. [CGWAVE results on the same grid using the rigorous procedure (3) were also obtained and found to be indistinguishable from the top of Fig. 4.] The new method reproduces the analytical solutions extremely well. Also, oscillations indicating artificial reflections from the open boundary are notably absent. Two other wave periods considered by Jonsson et al. (1976) were also modeled:  $T = 410$  s and  $T = 480$  s. As before, the results showed exceedingly small errors, and are hence not shown. These solutions are remarkable in view of the proximity of the open boundary to the island, and suggest that the new boundary conditions can accommodate the scattered waves satisfactorily.

The second test case concerns harbor problems, and the fre-

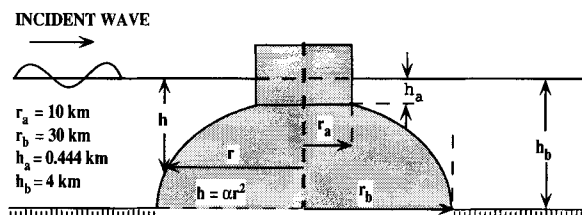


**FIG. 3. Bathymetry for Paraboloidal Shoal and Circular Island (after Jonsson et al. 1976)**

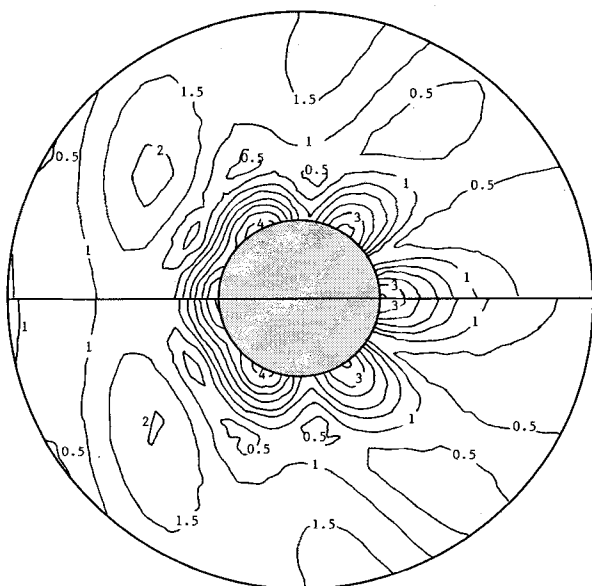


FIG. 4. Amplification Factors for Waves Incident from Left (Due to Symmetry, Results Only in Half Domain Are Shown: Top—Traditional Approach and Analytical Solutions (Results Nearly Identical); Bottom—Parabolic Boundary Conditions [Results Nearly Identical for (11) and (13)])

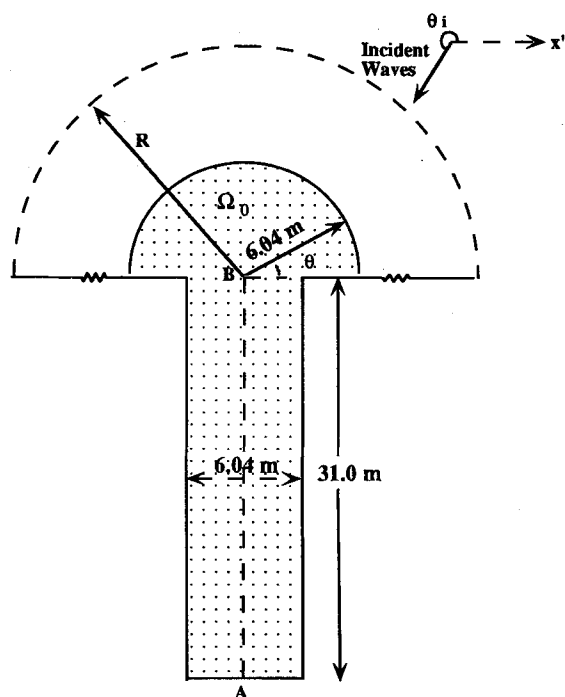


FIG. 5. Rectangular Harbor Model Domain

quently used rectangular harbor was considered (Fig. 5). With full reflection on all boundaries, the analytical resonance curve (Mei 1983) for the center of the back wall shows two peaks, corresponding to wave periods of approximately 11.1 s and 5.4 s, respectively. Since these resonant peaks are often difficult to simulate properly (Dong and Al-Mashouk 1989; Madsen and Larsen 1987; Panchang et al. 1991; Chen 1990), we will discuss results for these periods.

CGWAVE model results using the conventional and new methods were obtained for exterior reflectivities of 1 and 0.5. For convenience, the same reflectivities were assigned to the interior boundaries as well. For full reflection on all boundaries, the conventional method (3) is theoretically correct regardless of the location of the open boundary; its solution

along section AB (marked in Fig. 5) is shown in Fig. 6(a, b) for a wave period  $T = 11.1$  s. For the new method, however, the solution may be influenced by the location of the open boundary; it may be expected that scattering errors along section AB will diminish as the semicircle is placed far away from the harbor. This is borne out by Fig. 6(a and b), which shows the results obtained with (11) and (13), respectively, for

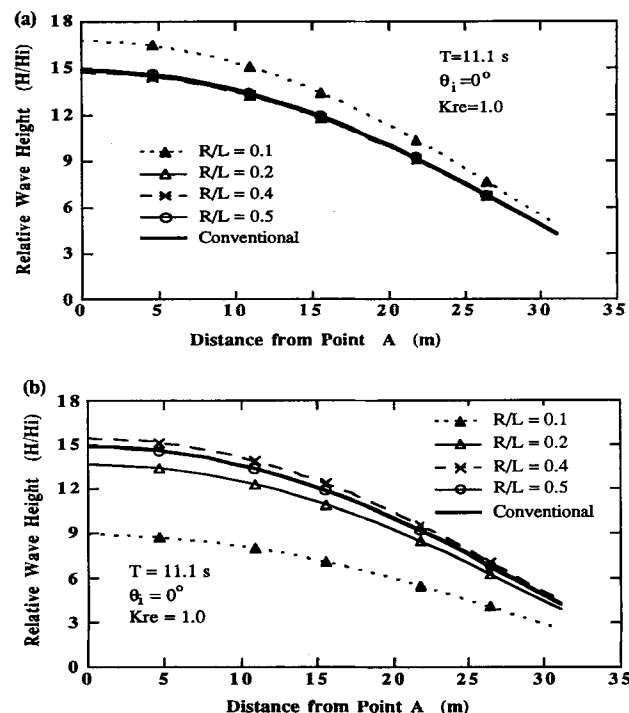


FIG. 6. Comparison of Amplification Factors, Fully Reflecting Boundaries,  $T = 11.1$  s: (a) Traditional Approach versus Parabolic Boundary Conditions, (11); (b) Traditional Approach versus Parabolic Boundary Conditions, (13)

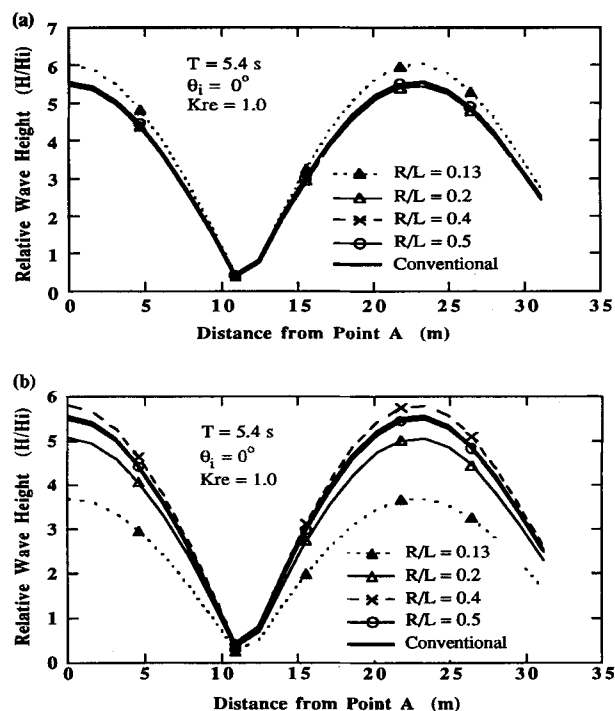


FIG. 7. Comparison of Amplification Factor, Fully Reflecting Boundaries,  $T = 5.4$  s: (a) Traditional Approach versus a Parabolic Boundary Conditions, (11); (b) Traditional Approach versus Parabolic Boundary Conditions, (13)

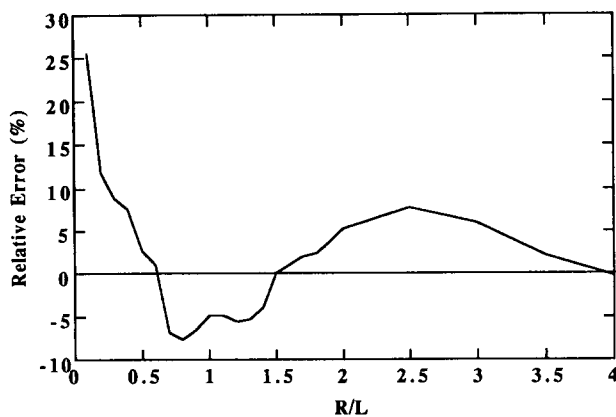


FIG. 8. Error in Amplification Factor at "B": True Solution Assumed to Be Given by Model Domain of Size  $R/L = 4.5$

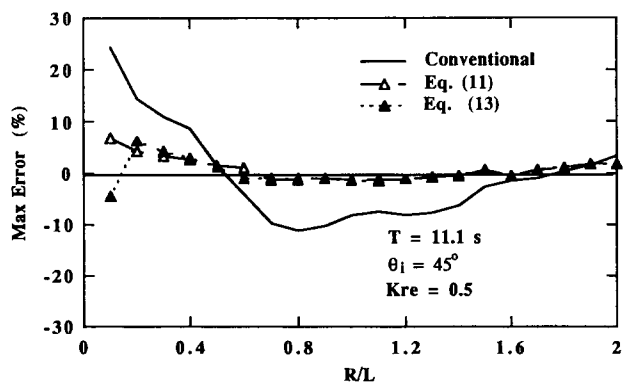
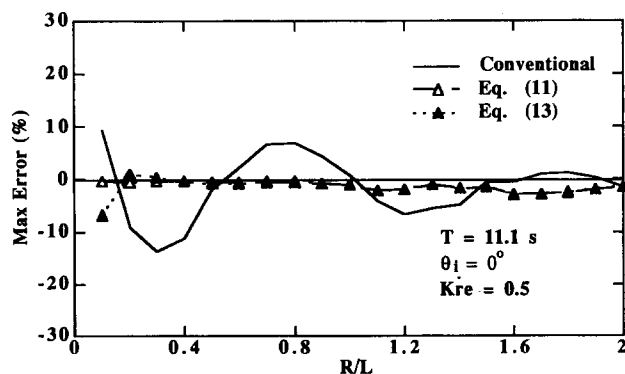


FIG. 9. Maximum Error in Amplification Factor along AB,  $T = 11.1$  s: (a) Incident Wave Angle =  $0^\circ$ ; (b) Incident Wave Angle =  $45^\circ$

domains of various sizes. While the expected convergence towards the conventional solution occurs for both methods, use of (11) is clearly superior. It is again remarkable, however, that even with  $R/L$  as small as 0.2, the solutions of the new methods are very close to the conventional solution. Similar results were obtained for  $T = 5.4$  s, as shown in Fig. 7(a, b).

Since most realistic coastal domains do not have fully reflecting exterior boundaries (as specified in the preceding paragraph), we also consider the case of the rectangular harbor (Fig. 5) with a reflection coefficient = 0.5 everywhere. The conventional method can be expected to yield reliable solutions only if  $R$  is sufficiently large so as not to influence the results at the region of interest (assumed here to be the dotted subdomain  $\Omega_0$  in Fig. 5). To obtain such a solution, 20 finite-element runs on domains of increasing size were made in the range  $0.1 < R/L < 2$ . The number of nodes varied from about 130 for the smallest domain to about 2,000 for the largest domain. It was found that the modeled wave heights in  $\Omega_0$  did

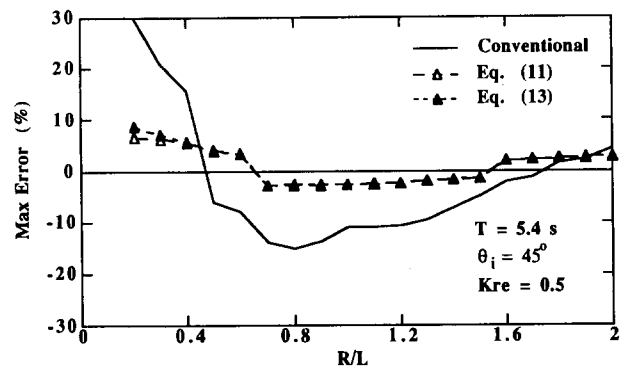
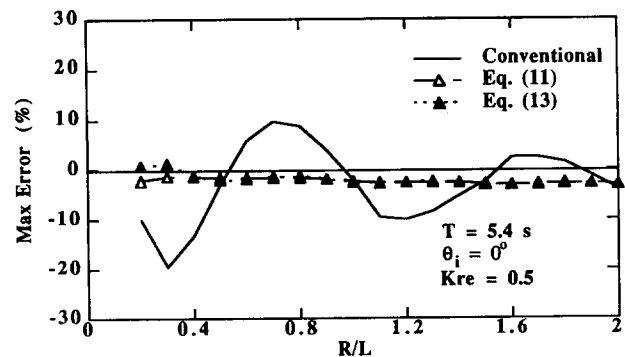


FIG. 10. Maximum Error in Amplification Factor along AB,  $T = 5.4$  s: (a) Incident Wave Angle =  $0^\circ$ ; (b) Incident Wave Angle =  $45^\circ$

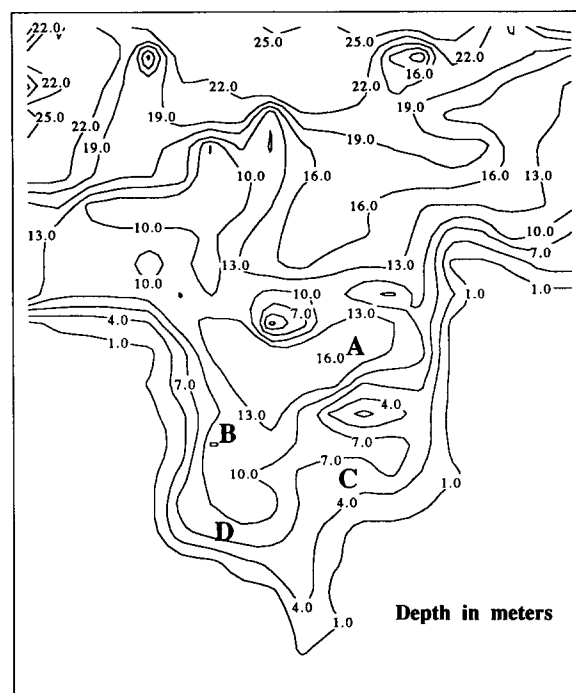


FIG. 11. Toothacher Bay Bathymetry

not converge monotonically as  $R$  increased. Instead, they oscillated, and the oscillations became smaller with increasing  $R$ . Extremely large domains were required to completely eliminate these oscillations, as shown in Fig. 8. For  $R/L > 1.6$  (approximately), the oscillations were generally smaller than 5%. The "true" solution was therefore constructed by averaging the results at each grid point in  $\Omega_0$  for the five largest model domains. Compared with this true result, the maximum errors in the wave height at any point in  $\Omega_0$  obtained from the conventional model using domains of varying sizes are shown

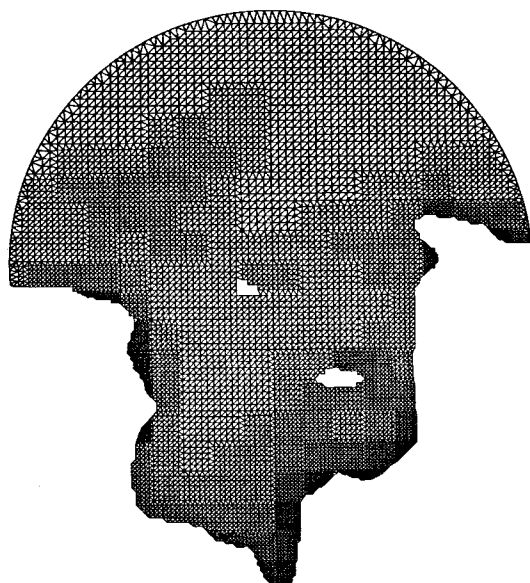


FIG. 12. Toothacher Bay Model Grid

in Fig. 9(a, b) for  $T = 11.1$  s and angles of incidence  $= 0^\circ$  and  $45^\circ$ . For comparison, maximum errors arising from the use of (11) and (13) are also shown in Fig. 9. It is clear that for a domain of a given size, the new method results in small errors, which are also generally much smaller than the errors stemming from the traditional approach. Also, these errors show far less sensitivity to  $R/L$  than the fluctuating errors with the traditional approach. These conclusions are reinforced by similar observations for  $T = 5.4$  s; see Fig. 10(a, b).

Wave propagation in Toothacher Bay was also simulated. The bathymetry and the model grid are shown in Figs. 11 and 12. More than 12,000 elements were used with a resolution of approximately  $L/7$  ( $L$  = local wavelength) for a period of  $T = 20$  s. The results of the traditional method were discussed earlier in the introduction (see Fig. 2). Wave heights at four locations marked, A, B, C, and D in Fig. 11 obtained by using the parabolic boundary conditions were compared with those obtained by the traditional approach. The differences were significant: 34%, 19%, 12%, and 7%, respectively. This shows that the influence of the traditional boundary conditions extend into the domain of interest. This influence is often even greater, and varies with angle of incidence and reflection coefficients along the boundaries. The overall results of the new method are shown in Fig. 13. These show a marked improvement in the quality compared with the simulations resulting from the traditional method which were shown earlier in Fig. 2. The parabolic boundary conditions are effective in eliminating the patches of large amplification factors resulting from the assumption of full exterior reflection in the traditional method. The phase pattern also shows a far more orderly pattern.

## CONCLUDING REMARKS

Traditional elliptic harbor wave models make certain assumptions regarding the exterior bathymetry to achieve a solution. When these assumptions are not met in practice (as is usually the case), model results often show a spurious and chaotic pattern with large waves, indicating that the effect of these assumptions cannot be ignored. Enlarging the computational domain to overcome these effects in the region of interest is usually not a viable option.

To overcome these difficulties, we have explored the use of parabolic approximations as open boundary conditions. This was first suggested by Kirby (1989) in the context of finite-difference rectangular domain models. In the present paper,

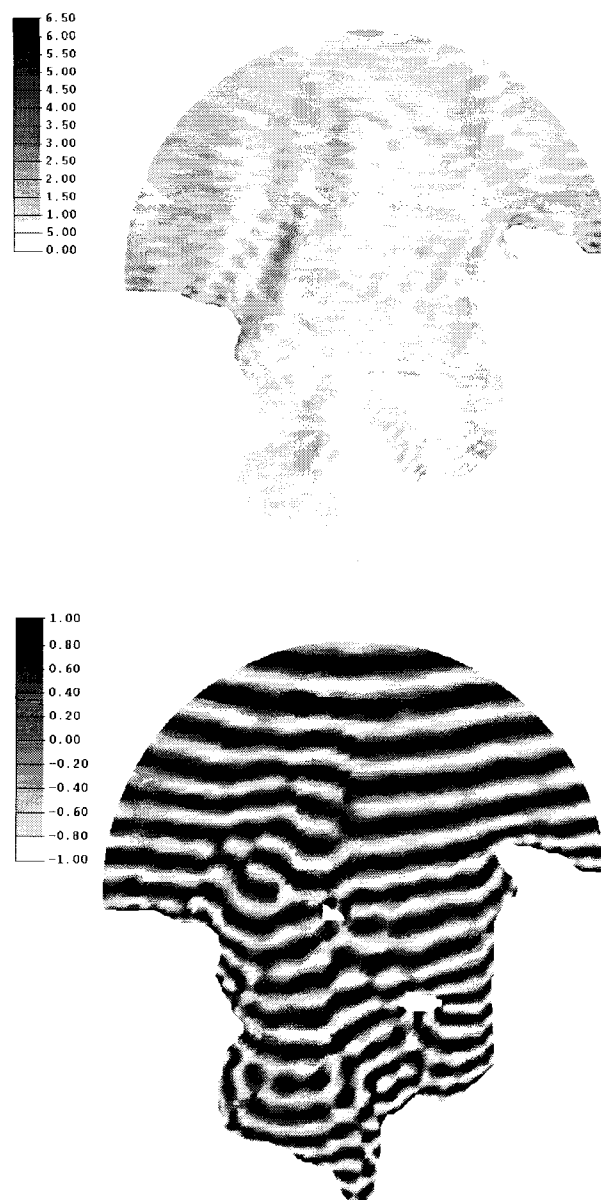


FIG. 13. Model Simulation in Toothacher Bay Using Parabolic Boundary Conditions: (a) Amplification Factors; (b) Cosine of Phase Angle

we have developed parabolic approximations in polar coordinates that are suitable for use as boundary conditions in elliptic finite-element models. The appropriate functional was developed to accommodate the parabolic boundary conditions in the solution of the mild-slope equation by the finite-element method. This functional was used in conjunction with the iterative techniques of Panchang et al. (1991) and Li (1994) and the grid-generator of Jones and Richards (1992) to construct a finite-element harbor wave model.

While the traditional method describes wave scattering completely (as long as the assumptions regarding the exterior geometry are met), the new boundary conditions that rely on parabolic approximations are limited in their ability to describe the scattered waves in all directions. The model was therefore tested against analytical solutions for the case of wave propagation around a circular island situated on a paraboloidal shoal. Since this bathymetry causes extensive scattering in all directions for long waves, it constitutes a rigorous test case for the parabolic boundary conditions. The results were found to be virtually identical to the analytical solutions. Further, the new method was compared with the classical method for a



rectangular harbor with fully reflecting walls (for which the latter method is rigorously correct). It was found that the modeled wavefield in the harbor was unaffected by the parabolic approximations even when the open boundary was placed quite close to the area of interest (viz.  $R/L \geq 0.2$  was found to be adequate). These tests suggest that the errors accruing from the parabolic boundary conditions are very small.

The new method was then applied to the more realistic case of partial reflection along the exterior boundary. For this case, the traditional method is not strictly applicable and a modeler would usually hope to obtain a reliable result by placing the open boundary very far from the area of interest. It was found that the results in this area ( $\Omega_0$ ) depend significantly on the location of the open boundary, and even with  $R/L > 4$ , complete convergence to the final solution was not obtained. This is partly due to the fact that the effects of full exterior reflection are not necessarily confined to the outer areas of  $\Omega$ ; rather, they are felt, to varying degrees, over all of the computational domain. The new method, on the other hand, produced (correct and) stable solutions with  $R/L \geq 0.2$ . This leads to significant savings in modeling effort (i.e. grid-generation, memory, central-processing-unit time, etc). The new method was also applied to Toothacher Bay and although no data are available for comparison, the results are far more acceptable from a qualitative standpoint than those of the conventional method.

Finally, it is noted that although the new method strictly speaking addresses only limitation 3 given in the introduction, by eliminating the need to have fully reflecting exterior boundaries, it indirectly addresses the limitation regarding the shape of the exterior coastline (i.e. limitation 2). As shown in Appendix I, a straight and collinear coastline is required in the traditional method in order to estimate the scattered potential  $\phi_s$  and the reflected wavefield  $\phi_r$ . In the new method, on the other hand, the scattered waves make no demand on the shape of exterior coastline; straightness is required only in order to estimate  $\phi_r$ . However, when the exterior reflectivity is low (a situation that the new method allows),  $\phi_r$  is likely to have a small effect on the overall solution (unlike the traditional approach where  $\phi_r$  perforce contains fully reflected waves). The new procedure hence enables the modeler to relax the requirement on the coastal geometry to some extent. However, as in the case of the traditional elliptic models and some parabolic equation models (Dalrymple and Martin 1992), the new procedure is still limited to constant depths in the exterior. This constant depth is usually judiciously selected as some average or representative depth along the open boundary. Efforts to eliminate this limitation will be described in a future paper.

## APPENDIX I.

The traditional treatment of exterior domains in harbor wave models is described in this appendix. Referring to Fig. 1, the exterior wavefield is written as  $\phi_{\text{ext}} = \phi_i + \phi_r + \phi_s$ , where  $\phi_i$ ,  $\phi_r$ , and  $\phi_s$  represent the incident, the reflected, and the scattered wavefields, respectively. If the water depth in the exterior is constant, the mild-slope equation (1) reduces to

$$\nabla^2 \phi + k^2 \phi = 0 \quad (22)$$

which is satisfied by  $\phi_i$ ,  $\phi_r$ , and  $\phi_s$ . As regards the scattered waves, the following solution of (22) may be found by separating variables:

$$\phi_s = \sum H_p(kr) [A_p \cos(p\theta) + B_p \sin(p\theta)] \quad (23)$$

where  $p$  = eigenvalue (to be determined); and  $H_p \equiv$  Hankel function of the first kind and order  $p$ . Using the asymptotic form of Hankel functions

$$H_p \sim \sqrt{\frac{2}{\pi kr}} \exp \left\{ i \left[ kr - \left( p + \frac{1}{2} \right) \frac{\pi}{2} \right] \right\} \quad \text{as } kr \rightarrow \infty \quad (24)$$

it is easy to show that  $\phi_s$  satisfies the following Sommerfeld radiation condition (Mei 1983):

$$\sqrt{kr} \left( \frac{\partial \phi_s}{\partial r} - ik \phi_s \right) \rightarrow 0, \quad \text{as } kr \rightarrow \infty \quad (25)$$

[Hankel functions of the second kind do not satisfy the Sommerfeld radiation condition at infinity and are hence excluded from (23).]

If the exterior coastlines are collinear, fully reflective, and lie along the  $x$ -axis, the boundary condition  $\partial \phi / \partial n = 0$  yields

$$\frac{\partial \phi_r}{\partial n} = -\frac{\partial \phi_i}{\partial n} \quad \text{along } \theta = 0 \quad \text{and } \theta = \pi \quad (26)$$

and

$$\frac{\partial \phi_s}{\partial n} = 0 \quad \text{along } \theta = 0 \quad \text{and } \theta = \pi \quad (27)$$

If  $\phi_i = A_i \exp[ikr \cos(\theta - \theta_i)]$ , one may use (26) to obtain  $\phi_r = A_i \exp[ikr \cos(\theta + \theta_i)]$ . To find  $\phi_s$ , substitute (23) into (27) along  $\theta = 0$

$$\frac{\partial \phi_s}{\partial n} = -\frac{1}{r} \frac{\partial \phi_s}{\partial \theta} = \sum -\frac{p}{r} H_p(kr) B_p = 0 \quad (28)$$

Hence  $B_p \equiv 0$ . Similar substitution along  $\theta = \pi$  gives

$$\sum -\frac{p}{r} H_p(kr) A_p \sin(p\pi) = 0 \quad (29)$$

which implies that  $\sin(p\pi) = 0$ . Thus the eigenvalue  $p$  is determined to be an integer (0, 1, 2, 3, ...).

If the boundary is partially reflecting, the boundary condition for  $\phi_s$  is

$$\frac{\partial \phi_s}{\partial n} = \alpha \phi_s \quad \text{at } \theta = 0 \quad \text{and } \theta = \pi \quad (30)$$

where  $\alpha$  is related to the reflection coefficient. Along  $\theta = 0$ , substitution of (23) into (30) gives the following relation:

$$\frac{p}{r} B_p + \alpha A_p = 0 \quad (31)$$

Since  $A_p$  and  $B_p$  are independent of  $r$ , for  $\alpha \neq 0$ , (31) holds only if  $A_p \equiv 0$  and  $B_p \equiv 0$ . Thus the traditional approach fails for a partially reflecting exterior boundary. Similarly collinear coastlines are also a requirement in order to obtain the preceding analytical solutions.

## ACKNOWLEDGMENTS

Partial support for this work was received from the U.S. Army Corps of Engineers (contract DAC 39-95-M-4459), the Maine Sea Grant College Program (National Oceanic and Atmospheric Administration, contracts NA36RG0110 and NA56RG0159), and from the University of Maine Center for Marine Studies. Assistance and comments provided by Prof. B. Cushman-Roisin of Dartmouth College are gratefully acknowledged.

## APPENDIX II. REFERENCES

- Berkhoff, J. C. W. (1976). "Mathematical models for simple harmonic linear water waves." *Wave refraction and diffraction*, Publ. 163, Delft Hydraulics Laboratory, Delft, The Netherlands.
- Chen, H. S. (1990). "Infinite elements for water wave radiation and scattering." *Int. J. Numer. Meth. in Fluids*, 11, 555-569.
- Chen, H. S., and Houston, J. R. (1987). "Calculation of water level oscillation in coastal harbors." *Instructional Rep. CERC-87-2*, Coast. Engrg. Res. Ctr., WES, Vicksburg, Miss.
- Dalrymple, R. A., and Martin P. A. (1992). "Perfect boundary conditions for parabolic water-wave models." *Proc., Royal Soc. London A*, London, U.K., 437, 41-54.
- Dong, P., and Al-Mashouk, M. (1989). "Comparison of transient and

- steady state wave models for harbor resonance." *Hydraulic and environmental modeling of coastal estuarine and river waters*, R. A. Falconer, P. Goodwin, and R. G. S. Matthew, eds., University of Bradford, Bradford, U.K.
- Hom-ma, S. (1950). "On the behaviour of seismic sea waves around circular island." *Geophys. Mag.*, 21, 199.
- Houston, J. R. (1981). Combined refraction and diffraction of short waves using the finite element method." *Appl. Oc. Res.*, 3(4), 163–170.
- Isobe, M. (1986). "A parabolic refraction-diffraction equation in the ray-front coordinate system." *Proc. 20th Int. Conf. Coast. Engrg.*, Taipei, Taiwan, 306–317.
- Jones, N. L., and Richards, D. R. (1992). "Mesh generation for estuarine flow models." *J. Wtrwy., Port, Coast., and Oc. Engrg.*, ASCE, 118(6), 599–614.
- Jonsson, I. G., Skovgaard, O., and Brink-Kjaer, O. (1976). Diffraction and refraction calculations for waves incident on an island." *J. Marine Res.*, 34, 469–496.
- Kirby, J. T. (1986a). Higher-order approximations in the parabolic equation method for water waves." *J. Geophys. Res.*, 91, C1, 933–952.
- Kirby, J. T. (1986b). "Rational approximations in the parabolic equation method for water waves." *Coast. Engrg.*, 10, 355–378.
- Kirby, J. T. (1988). "Parabolic wave computations in non-orthogonal coordinate systems." *J. Wtrwy., Port, Coast., and Oc. Engrg.*, ASCE, 114(6), 673–685.
- Kirby, J. T. (1989). "A note on parabolic radiation boundary conditions for elliptic wave calculations." *Coast. Engrg.*, 13, 211–218.
- Kirby, J. T., Dalrymple, R. A., and Kaku, H. (1994). "Parabolic approximations for water waves in conformal coordinate systems." *Coast. Engrg.*, 23, 185–213.
- Kostense, J. K., Meijer, K. L., Dingemans, M. W., Mynett, A. E., and van den Bosch, P. (1986). "Wave energy dissipation in arbitrarily shaped harbours of variable depth." *Proc. 20th Int. Conf. Coast. Engrg.*, 2002–2016.
- Li, B. (1994). A generalized conjugate gradient model for the mild slope equation." *Coast. Engrg.*, 23, 215–225.
- Liu, P. L.-F., and Boissevain, P. L. (1988). "Wave propagation between two breakwaters." *J. Wtrwy., Port., Coast., and Oc. Engrg.*, ASCE, 114(2), 237–247.
- Madsen, P. A., and Larsen, J. (1987). "An efficient finite-difference approach to the mild-slope equation." *Coast. Engrg.*, 11, 329–351.
- Mei, C. C. (1983). *The applied dynamics of ocean surface waves*. John Wiley, New York, N.Y.
- Panchang, V. G., Cushman-Roisin, B., and Pearce, B. R. (1988). "Combined refraction-diffraction of short waves for large domains." *Coast. Engrg.*, 12, 133–156.
- Panchang, V. G., Pearce, B. R., Ge, W., and Cushman-Roisin, B. (1991). "Solution to the mild-slope wave problem by iteration." *Appl. Oc. Res.*, 13(4), 187–199.
- Panchang, V. G., Xu, B., and Cushman-Roisin, B. (1993). "Bathymetric variations in the exterior domain of a harbor wave model." *Proc. Int. Conf. Hydroscl. & Engrg.*, S. Wang, ed., Washington, D.C., 1555–1562.
- Radder, A. C. (1979). "On the parabolic equation method for water-wave propagation." *J. Fluid Mech.*, 95, 159–176.
- Tsay, T.-K., and Liu, P. L.-F. (1982). "Numerical solution of water-wave refraction and diffraction problems in the parabolic approximation." *J. Geophys. Res.*, 87, C10.
- Tsay, T.-K., and Liu, P. L. F. (1983). "A finite element model for wave refraction and diffraction." *Appl. Oc. Res.*, 5(1), 30–37.
- Xu, B., and Panchang, V. G. (1993). "Outgoing boundary conditions for finite-difference elliptic water-wave models." *Proc., Royal Soc. of London, Series A*, London, U.K., 441, 575–588.